

BEHAVIOR OF DEFORMED BARS ANCHORED AT INTERIOR
JOINTS UNDER SEISMIC EXCITATIONS

by

R. Eligehausen¹⁾, E.P. Popov²⁾ and V.V. Bertero²⁾

SUMMARY

A mathematical model of a deformed bar anchored at interior joints of ductile moment resisting reinforced concrete frames subjected to severe earthquakes is presented. It includes the formulation of an accurate model for the local bond stress-slip relationship, use of a simple model for the stress-strain relationship of the reinforcing steel and the numerical solution of the differential equation of bond. The analytically predicted response of anchored beam bars compares well with the results of a series of tests for monotonic and cyclic loading. The influence of major parameters of the behavior of anchored bars is shown by an extensive numerical study. The results of this investigation are used to offer practical recommendations for the anchorage of beam bars at interior joints.

I. INTRODUCTION

Under severe seismic excitations, the hysteretic behavior of reinforced concrete structures appears to be highly dependent on the interaction between steel and concrete. Tests show that when the developing story displacement ductility ratio is four or more, fixed end rotations caused by slip of the main steel bars along their embedment length in beam-column joints may contribute up to 50 percent to the total beam deflection. This contribution must be fully understood and included in the analytical prediction of response. However, in spite of recent integrated experimental and analytical studies devoted to investigating this problem (1), no reliable bond stress-slip laws for generalized excitations are available (2). Therefore extensive experimental and analytical investigations were carried out at Berkeley with the aim to obtain a better insight into the behavior of anchored beam bars. In this paper the work reported in (3-7) is summarized.

II. MATHEMATICAL MODEL

The behavior of a bar of finite length embedded in a concrete block is idealized as a one-dimensional problem and modeled using the non-linear differential equation of bond (Fig. 1). The equation connects the axial force in the bar, N , to the bond stresses, τ , on the perimeter of the bar. It has to be coupled with the constitutive laws for steel and bond. The differential equation together with the specified boundary conditions at

1) Senior Research Engineer, University of Stuttgart, West Germany

2) Professor of Civil Engineering, University of California, Berkeley

the two end points of the bar (Fig. 2) define a non-linear two point boundary value problem. This was solved here by transforming the boundary value problem into an initial value problem (shooting technique) (7).

2.1 Steel Model

Two models were used for the stress-strain relationship of the bar in alternative (Fig. 3). The bilinear model is very simple and computationally very economical. However, it neglects the Bauschinger effect. Therefore the non-linear model was used as well. The stress-strain relationship is described by a non-linear equation proposed in (8) (see Fig. 3) and a set of simplified rules used in (9) which allow sufficiently accurate reproduction of the bar behavior under generalized strain histories.

2.2 Local Bond Model

The local bond model was derived from results of an extensive experimental study. The basic design of the test specimen representing the confined region of a beam-column joint is shown in Fig. 4. The bonded length of a Grade 60 deformed bar was limited to $5 d_b$. The horizontal concrete splitting area associated with the embedded bar was controlled by the size of the opening in the plastic sheet. By varying the width of the opening in this sheet, simulation of different bar spacings was achieved. The test specimen was installed in a specially designed testing frame (Fig. 5) and was loaded by a hydraulic servo-controlled universal testing machine. The tests were run under slip control by subjecting the threaded loading end of the bar to the required force needed to induce the desired slip measured at the unloaded bar end. Some 125 specimens were tested. The effects of the following variables on the local bond stress-slip relationship were studied: 1) Monotonic vs. cyclic loading with varying slip histories, 2) tensile vs. compressive loading, 3) amount of confinement reinforcement, 4) bar diameter, 5) concrete strength, 6) bar spacing, 7) transverse pressure and 8) rate of pull-out.

Specimens without secondary reinforcement failed by splitting of the concrete in the plane of the tested bar. The concrete between ribs was undamaged (Fig. 6). Splitting cracks were also observed in the other tests, however, their growth was controlled by the confining reinforcement. Failure was caused by bar pull-out. The concrete between the bar ribs was completely sheared off and pulverized (Fig. 7).

Typical test results are shown in Figs. 8 and 9. Plotted are the calculated average local bond stress as a function of the slip at the unloaded bar end. Several interesting aspects can be observed from these diagrams. 1) The monotonic bond stress-slip relationship for loading in tension is almost identical to that for loading in compression. 2) The descending branch of the bond stress-slip curve levels off to an almost constant bond stress at a slip approximately equal to the clear distance between lugs. 3) If the peak bond stress during cycling does not exceed about 70 percent of the monotonic bond strength, the ensuing bond stress-slip relationship at slip values larger than the one at which the specimen was cycled is not significantly influenced by up to 10 cycles (Fig. 8). 4) After loading the specimen to slip values inducing a bond stress larger

than about 70 percent of the monotonic bond strength, a significant reduction in bond capacity takes place even during the first slip reversal (Fig. 9). After one cycle the bar bond capacity does not reach the monotonic loading curve. Bond damage continues under further application of cyclic loading and increases with increasing peak slip values. 5) Frictional resistance during cyclic loading deteriorates rapidly with increasing number of cycles.

Another significant result was that the behavior of bond during cyclic loading was not much influenced by the various parameters investigated, if the deterioration of bond resistance was related to the pertinent monotonic envelope.

The analytical bond model deduced from the test results described above is shown in Fig. 10. It was first presented in (5) and consists of a monotonic envelope, reduced envelope, unloading-, friction- and reloading branch. Some information about the different branches are given in the following. A complete description can be found in (4).

The monotonic envelope consists of an initial non-linear relationship, followed by a plateau and a linearly decreasing branch. For slip values larger than the clear distance between the lugs of the deformed bars the bond stress is assumed to be constant and equal to the ultimate frictional bond resistance.

Reduced envelopes are obtained from the monotonic envelope by reducing the characteristic bond stresses through a "damage parameter" d . For no damage, $d = 0$, the reloading branch reaches the monotonic envelope. For full damage, $d = 1$, bond is completely destroyed ($\tau = 0$). It is assumed that the deterioration of bond stiffness and bond strength during cyclic loading is caused by damage of the concrete between lugs which in turn is a function of the dissipated energy. The assumption that damage is related to the dissipated energy is theoretically acceptable in the range of low cycle fatigue.

The frictional bond resistance after first unloading depends upon the peak value of slip and is related to the value of the ultimate frictional bond resistance of the corresponding reduced envelope. For subsequent cycles, the frictional bond resistance is deduced from this initial value by multiplying it with an additional reduction factor which depends on the energy dissipated by friction alone.

The slope of the unloading and reloading branch is assumed as constant. Values for the parameters defining the bond model valid for various bond conditions are given in (4). With these values the analytical bond model was successful in reproducing the results of the above described tests with sufficient accuracy for practical purposes (Fig. 11).

Recently the analytical bond model was improved (10) insofar as the reloading branch starts well before reaching the peak slip value during cycling and its slope is much lower than in the model described above (see dotted line in Fig. 10). With this improvement the agreement between analytical and experimental results is even better than shown in Fig. 11.

The constitutive bond model presented so far is valid only for deformed bars embedded in well confined concrete. However, the bond conditions vary along the bar embedment length. For an interior joint three different regions have been identified in (1) (see Fig. 12). They show differences both in the shape of the monotonic envelopes, different for positive and negative slip, and in the rate of bond degradation. These differences are caused by the early formation of a concrete cone at the tensioned bar end and by transverse pressure on the bar at the compressed bar end. To cover this behavior which significantly influences the behavior of beam bars anchored in joints, the analytical bond model was modified and varying bond laws along the embedment length were specified. Details are given in (4,7).

2.3 Comparison of analytical predictions of the response of anchored bars with test results

The accuracy of the mathematical model referred to above has been checked by applying it to some bond tests with long embedment length (1). In those tests the diameter of the bar was $d_b \sim 25$ mm, the anchorage length $l_d = 25 d_b$ and the concrete strength $f'_c \sim 30$ N/mm². The characteristic values for the local bond stress-slip relationships along the embedment length were deduced from the results of the experimental study described in Section 2.2 and were taken from (4). Two of such analytical comparisons for a bar loaded by a tension and compression force of equal magnitude at the bar ends are shown in Figs. 13 and 14. The agreement between the calculated force-displacement relationships for one bar end and the experimental results seems to be acceptable for practical purposes. However, during cyclic loading the reloading branch of the analytical prediction is stiffer than measured in the experiment. When using the improved local bond model, this slight disadvantage is overcome (10).

III. NUMERICAL STUDIES

The influence of major parameters on the behavior of anchored beam bars was investigated by calculating the model response to imposed histories of displacements (slip), just as it would be done in an experiment. In most of the numerical studies, a 25 mm bar was pulled and pushed with forces of equal magnitude to simulate conditions at an interior joint. In the calculations the "old" bond model was used. The assumed bond behavior along the embedment length was the same as in Section 2.3.

3.1 Model for stress-strain relationship of reinforcing bar

Fig. 15 shows the influence of the steel model (bilinear or non-linear) on the calculated response of a bar loaded at one end only and subjected to reversed slip with increasing amplitude. As can be seen, the overall response is not much influenced by the different steel models. Therefore in the following studies the bilinear steel model was adopted.

3.2 Severity of hysteretic requirements

In this series of numerical tests the anchorage length and the steel characteristics were held fixed in order to study the influence of different loading histories. They consisted of reversed cycles between con-

stant slip values, which were chosen to give specified steel strains under monotonic loading. The peak steel strains varies between $\xi = \pm \xi_y$ (ξ_y = yield strain) and $\xi = \pm 30$ mm/m.

In Fig. 16 the normal force-slip relationships are plotted for the studied extreme cases: a) 6 cycles with peak steel strain value $\xi = \pm \xi_y$ (= 2.2 mm/m) and b) 3 cycles with $\xi = \pm 15$ mm/m followed by 3 cycles with $\xi = \pm 30$ mm/m. For comparison the response of the anchored bar under monotonic loading is shown as well. Even cycling between slip values corresponding to peak steel strains $\xi = \pm \xi_y$ leads to a considerable reduction of the maximum resistance and the deformability at maximum resistance compared to monotonic loading (Fig. 16a). This is mainly caused by the reduction of bond resistance at the compressed bar end (see Fig. 16c) due to the formation of a concrete cone during previous loading in tension. With increasing hysteretic requirements stiffness and strength of the anchorage are increasingly reduced. The maximum resistance of the anchored bar after some cycles between slip values corresponding to peak steel strains which might be expected during a strong earthquake amounts to only about 25 percent of the strength under monotonic loading (Fig. 16b).

3.3 Yield strength of steel

In this set of numerical tests the anchorage length was $25 d_b$ and the loading history was the same as in case b) of Section 2.2. The yield strength f_y was varied between 300 N/mm^2 and 600 N/mm^2 . The main results are plotted in Fig. 17.

Under monotonic loading (Fig. 17a) the anchorage force increases with increasing yield strength for slip values $s_1 < 4$ mm. However, the strength of the anchorage is almost independent of f_y . The deterioration of the anchorage resistance caused by cyclic loading increases significantly with increasing yield strength. While for the given conditions the deterioration is small for bars with $f_y = 300 \text{ N/mm}^2$ (Fig. 17b), the bond of bars with $f_y = 600 \text{ N/mm}^2$ is almost completely damaged by some cycles (Fig. 17c).

3.4 Anchorage length

The influence of the anchorage length on the bar response was studied using the same steel characteristics as in Section 3.2 and hysteretic requirements as given in Section 3.3. The main results are plotted in Fig. 18.

The hysteretic loops of anchorages with $l_d = 25 d_b$ are significantly pinched (see Fig. 16b), because the bond is severely damaged along the entire embedment length. This can be seen from Fig. 18b, which shows the distribution of slip along the anchorage length for a peak slip at the tensioned bar end of 5 mm. When considering that for the assumed concrete strength a shear failure of the concrete keys between lugs is initiated for slip values $s > 1$ mm (4), Fig. 18b clearly indicates this type of bond failure along the entire anchorage length after cyclic loading. Anchorages with a length of $35 d_b$ show almost stable hysteretic loops (Fig. 18a) and no bond damage along the inner parts of the anchorage length (Fig. 18c).

IV. PRACTICAL IMPLICATIONS OF RESULTS

From the results obtained in the numerical studies the necessary anchorage length of main beam bars at interior joints of ductile moment resistant R/C frames can be deduced. This length is significantly influenced by hysteretic requirements, required performance of the anchorage during cyclic loading and actual yield strength. These problems are discussed in detail in (7). To minimize effects of slip on the dynamic response of R/C frames under strong ground motions, an anchorage length of approximately $25 d_b$ or $35 d_b$ is necessary for Grade 40 ($f_y \sim 275 \text{ N/mm}^2$) or Grade 60 ($f_y \sim 415 \text{ N/mm}^2$) deformed bars respectively. These values are valid for a specified concrete strength $f'_c = 30 \text{ N/mm}^2$. The recommended anchorage lengths agree well with the values proposed in (11).

If the width of columns at interior joints is smaller than the proposed anchorage length, the formation of plastic hinges in girders near column faces should be avoided by detailing the reinforcement in an appropriate manner to avoid excessive slip and damage of bond. This is in accordance with earlier recommendations (12). Otherwise the influence of slip of main beam bars on the dynamic response of ductile moment resisting R/C frames under strong ground motions may become too important to be neglected in the analysis. The analytical model presented herein was used to formulate simplified joint models, which realistically take into account the influence of slip (13).

V. CONCLUSIONS

From the results obtained in this study the following main observations can be made:

- (1) The proposed mathematical model allows to predict with accuracy sufficient for practical purposes the response of deformed reinforcing bars anchored at interior joints of ductile moment resisting reinforced concrete frames under generalized excitations.
- (2) Under otherwise constant conditions, the deterioration of bond resistance during cyclic loading increases with increasing hysteretic requirements (intensity of strain and number of cycles), increasing yield strength and decreasing anchorage length.
- (3) The performance of anchorages can be significantly improved by choosing bars with a low yield stress.
- (4) Practical recommendations for the design of anchorages at interior joints are given.

REFERENCES

- (1) Vivathanatepa, S., Popov, E.P. and Bertero, V.V.: Effects of Generalized Loadings on Bond of Reinforcing Bars Embedded in Confined Concrete Blocks; Report No. UCB/EERC-79/22, Earthquake Engineering Research Center, University of California, Berkeley, 1979

- (2) Tassios, T.P.: Properties of Bond Between Concrete and Steel Under Load Cycles Idealizing Seismic Actions; Bulletin d'Information No. 131 of the Comité Euro-International du Béton, Paris, April 1979
- (3) Eligehausen, R., Popov, E.P. and Bertero, V.V.: Local Bond Stress Slip Relationships of Deformed Bars Under Generalized Excitations; Proceedings, Seventh European Conference on Earthquake Engineering, Volume 4, p. 69-80, 1982
- (4) Eligehausen, R., Bertero, V.V. and Popov, E.P.: Local Bond Stress-Slip Relationships of Deformed Bars Under Generalized Excitations, Tests and Analytical Model; Report No. UCB/EERC-83, Earthquake Eng. Research Center, University of California, Berkeley
- (5) Ciampi, V., Eligehausen, R., Bertero, V.V. and Popov, E.P.: Analytical Model for Deformed Bar Bond Under Generalized Excitations, Proceedings, IABSE Colloquium on Advanced Mechanics of Reinforced Concr., Delft, p. 53-67, June 1981
- (6) Ciampi, V., Eligehausen, R., Bertero, V.V. and Popov, E.P.: Hysteretic Behavior of Deformed Reinforcing Bars Under Seismic Excitations; Proceedings, Seventh European Conference on Earthquake Engineering, Vol. 4, p. 179-187, Athens, 1982
- (7) Ciampi, V., Eligehausen, R., Bertero, V.V. and Popov, E.P.: Analytical Model for Concrete Anchorages of Reinforcing Bars Under Generalized Excitations; Report No. UCB/EERC-82/23, Earthquake Engineering Research Center, University of California, Berkeley, 1982
- (8) Giuffrè, A. and Pinto, P.E.: Reinforced Concrete Behavior Under Strong Repeated Loadings; G. Genio Civile, No. 5, 1970 (in Italian)
- (9) Capecchi, D., Ciampi, V. and Vestroni, F.: Numerical Studies on the Behavior of a Reinforced Concrete Beam Element Under Repeated Loadings; Bulletin d'Information No. 132 of the Comité Euro-International du Béton, p. 105-113, Paris, April 1979
- (10) Eligehausen, R.: Improved Analytical Model for the Local Bond Stress-Slip Relationship of Deformed Bars Under Generalized Excitations; Report of the Institute for Material Science, University of Stuttgart, 1983, in final stage of preparation
- (11) Park, R.: Accomplishments and Research and Development Needs in New Zealand; Proceedings, Workshop on Earthquake-Resistant Reinforced Concrete Building Construction, University of California, Vol. II, July 1977
- (12) Galunic, B., Bertero, V.V. and Popov, E.P.: An Approach for Improving Seismic Behavior of Reinforced Concrete Interior Joints; Earthquake Engineering Research Center, University of California, Berkeley, Report No. UCB/EERC-77/33, December 1977
- (13) Filippou, F., Popov, E.P. and Bertero, V.V.: Mathematical Modeling of R/C Joints Under Cyclic Excitations; Journal of the Structural Division, ASCE, in review

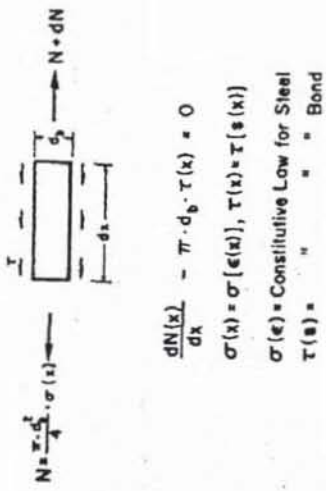


Fig. 1: Differential equation of bond of bond

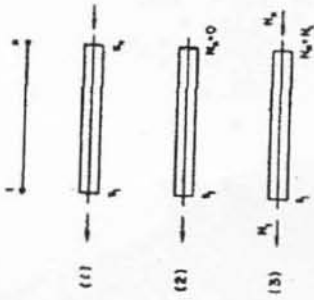


Fig. 2: Boundary conditions considered in the program

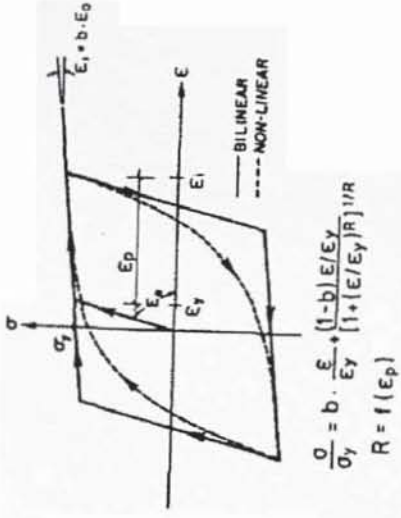


Fig. 3: Steel models

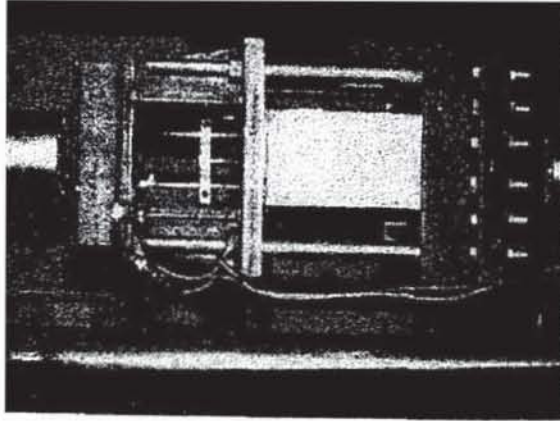


Fig. 5: Photo illustrating test set-up

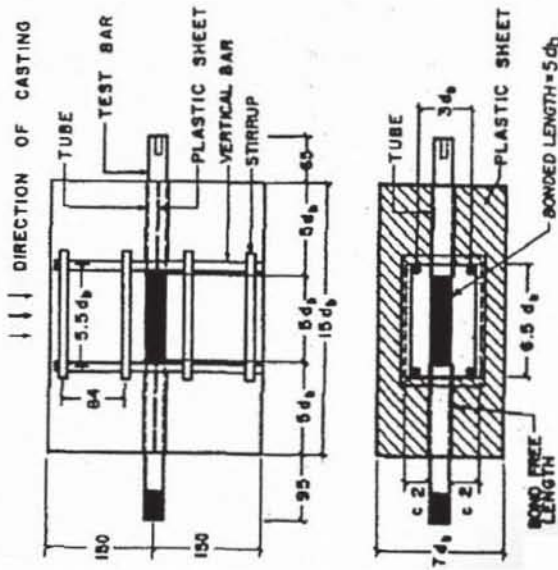


Fig. 4: Test specimen

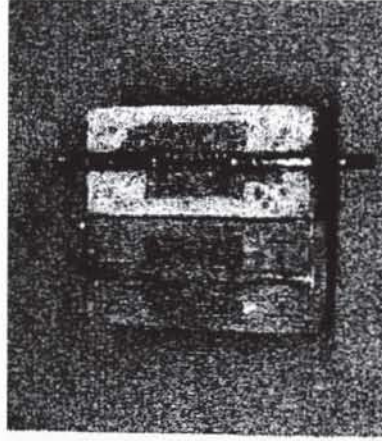


Fig. 6: Specimen failed by splitting

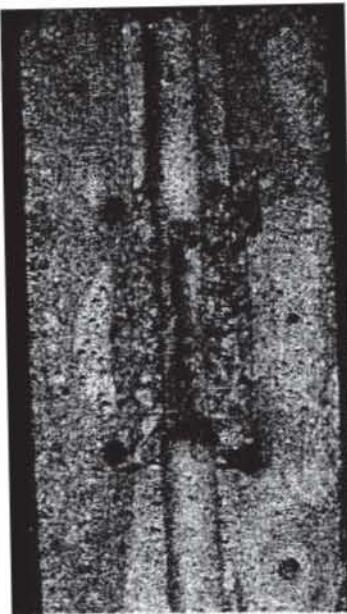


Fig. 7: Specimen failed by pullout

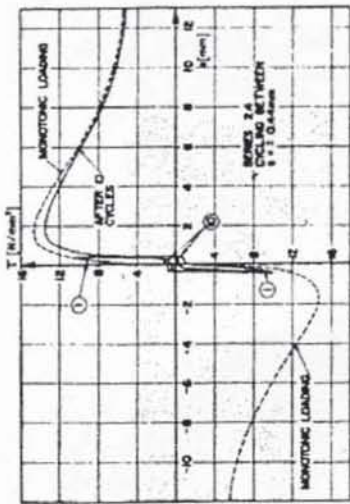


Fig. 8: Test result, cycling between $s = \pm 0,44$ mm

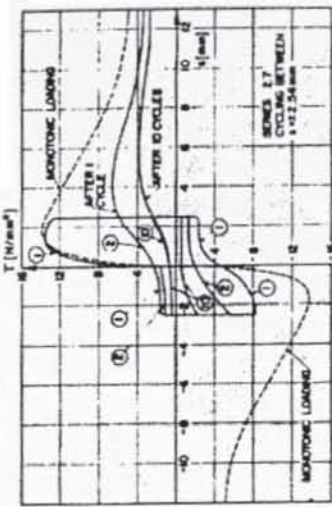


Fig. 9: Test result, cycling between $s = \pm 2,54$ mm

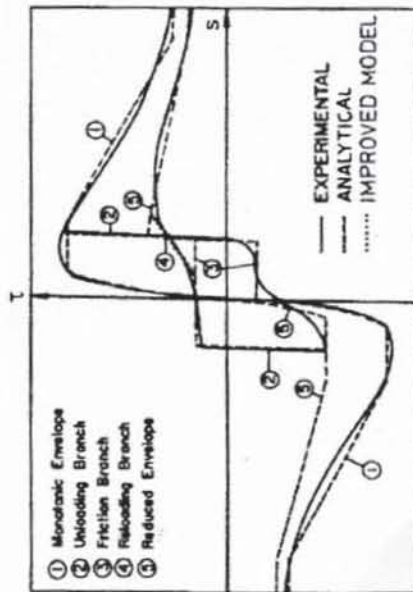


Fig. 10: Analytical model for local bond stress-slip relationships

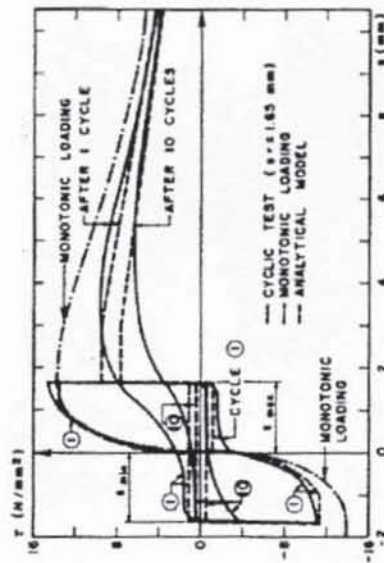


Fig. 11: Comparison of experimental and analytical results on local bond stress-slip relationships

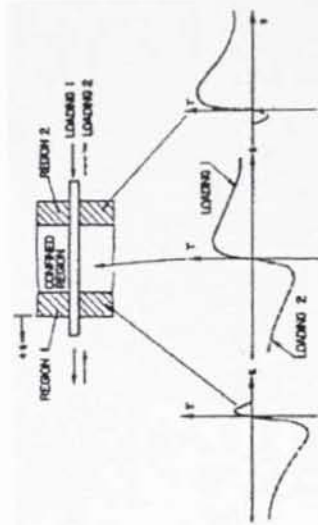


Fig. 12: Bond stress-slip relationships under monotonic loading for different regions in a joint

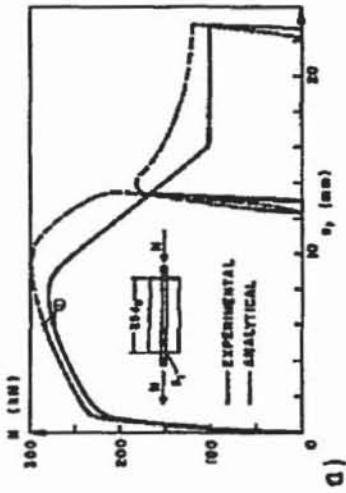


Fig. 13: Comparison of experimental results, test 13 of (1)

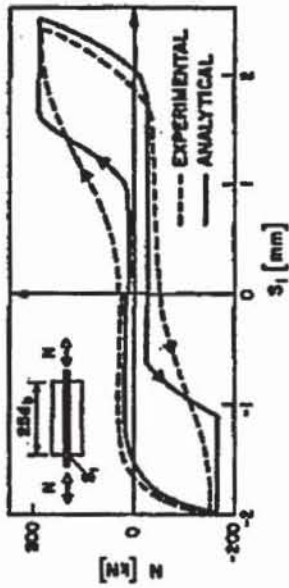


Fig. 14: Comparison of experimental and analytical results, cycle 21 of test 14 (1)

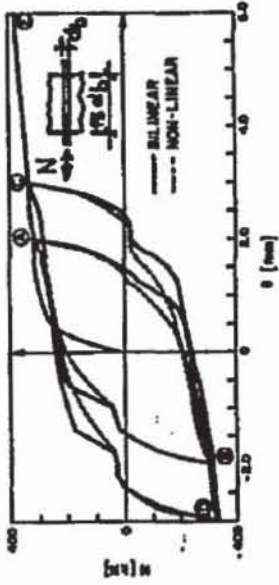
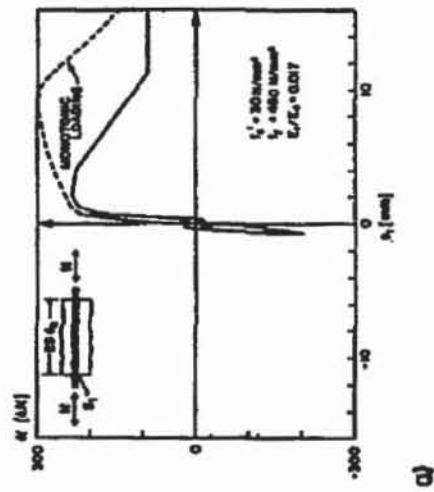
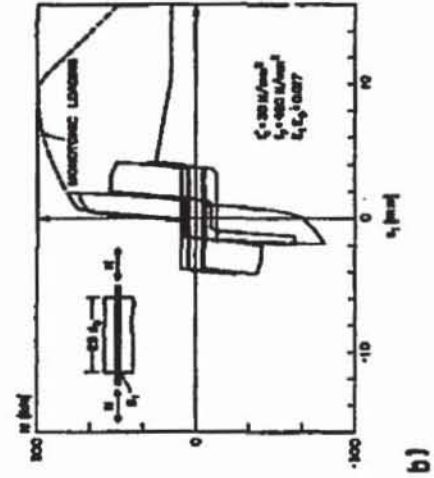


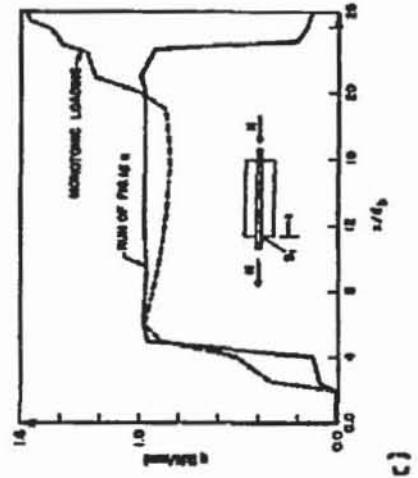
Fig. 15: Influence of steel model on the response of anchored beam bar



a)



b)



c)

Fig. 16: Influence of hysteretic requirements on the response of anchored beam bars

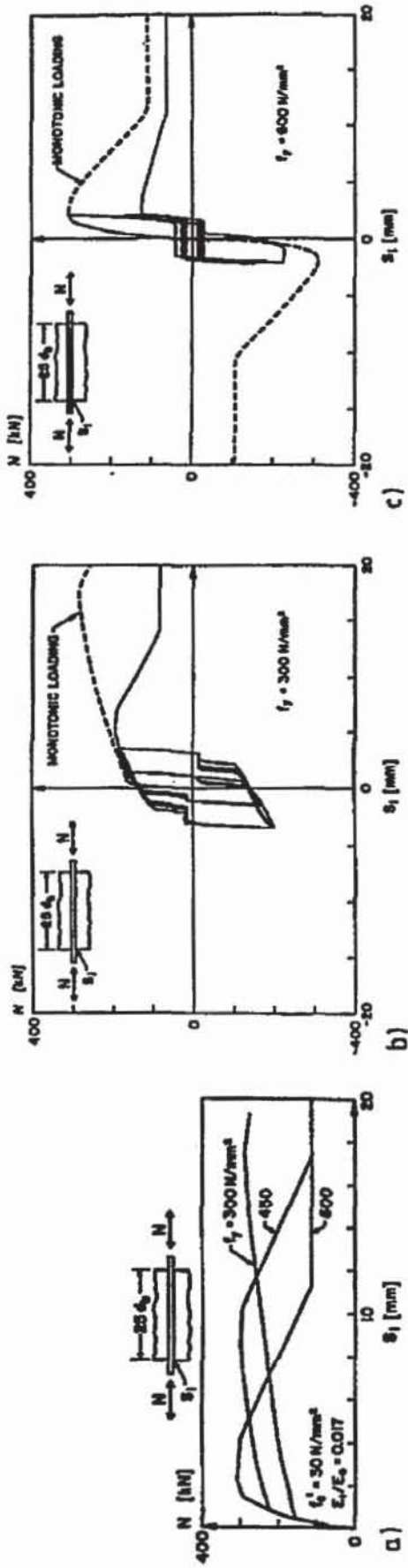


Fig. 17: Influence of yield stress on the response of anchored beam bars

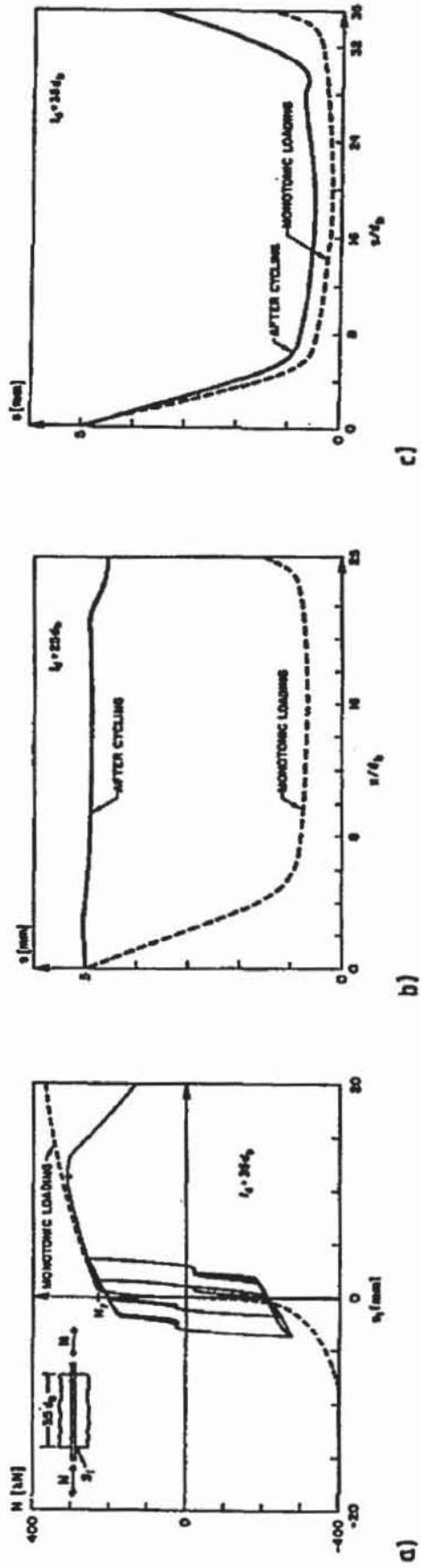


Fig. 18: Influence of anchorage length on the response of anchored beam bars